CHEMISTRY
A EUROPEAN JOURNAL

DOI: 10.1002/chem.201000053

Selective Gas Adsorption in the Flexible Metal–Organic Frameworks Cu(BDTri)L (L = DMF, DEF)

Aude Demessence and Jeffrey R. Long*[a]

Abstract: Use of the ditopic ligand 1,4-benzenedi(1*H*-1,2,3-triazole) (H_2BDTri) enabled isolation of two new three-dimensional metal–organic frameworks of formulae Cu(BDTri)L in which L = DMF (**1**) and diethylformamide (DEF; **2**). These compounds have the same primary structure, featuring one-dimensional channels with the bridging DMF or DEF molecules pointing into the cavity. Upon exposure to solvent vapors, both display a reversible flexibility, as characterized by single-crystal to single-crystal phase transitions in **1**. The O_2 adsorption isotherms for the compounds show a two-step adsorption behavior associated with a permanent microporosity and a pore-opening process. In the case of N_2 adsorption, only **1** exhibits a two-step adsorption isotherm, whereas **2** does not present any pore opening, demonstrating that design of a flexible framework cavity can control the pore opening and thereby possibly enhance O_2/N_2 separation.

Keywords: adsorption · metal–organic frameworks · porous materials · triazoles

Introduction

Flexible metal–organic frameworks have attracted much attention for their "breathing" structures and unusual properties in response to guest adsorption.[1] This structural dynamism has led to studies of selective gas adsorption,[2] molecular accommodation,[3] sensing,[4] and the kinetics of (multi)-stepwise gas adsorption.[5] Associated with the flexibility of the framework, such materials often exhibit gas selectivity by a stepwise adsorption caused by a guest-induced framework transition. Besides size or shape exclusion and adsorbate–surface interaction characteristics of rigid frameworks, dynamic frameworks show structural rearrangements during adsorption–desorption processes. These structural transformations are guest dependant and, interestingly, can lead to control of the selectivity over several adsorbates.[6] In particular, small gaseous adsorbates, such as O_2 and N_2, are attractive targets for research, first because the differences in sorption behavior between such similar gas molecules have attracted commercial interest for processes such as air separation, but also because of scientific interest as a result of their simple structures and small differences in physical properties.[7] To selectively adsorb gas molecules with very similar kinetic diameters in a flexible framework, the approach is to modulate the pressure of the pore opening by tuning the internal surface of the host. The conventional ways to modulate pore surfaces is to chemically elaborate the frameworks through incorporation of functional ligands, inclusion of metal salts, adjustment of the charge, or addition of water molecules.[2a,8] Removing or changing the coordinated solvent molecules through a postsynthetic approach is also a common strategy used to control the gas adsorption selectivity in rigid metal–organic frameworks.[9] Recognizing the promise of effects induced by coordinated solvent molecules, we have attempted to apply this strategy within a series of flexible frameworks to modulate the gate opening for O_2/N_2 gas separation.

In the design and synthesis of flexible porous materials with new structural topologies and high thermal and chemical stabilities, carboxylate- and pyridine-based ligands have been used extensively. Azolate-based bridging ligands, however, have recently attracted interest as a means of generating frameworks with surfaces featuring solvated metal sites.[10] To obtain a high symmetry bridging ligand and new triazolate-based frameworks, we developed the synthesis of a ditopic ligand with a 1*H*-1,2,3-triazole function, namely 1,4-benzenedi(1*H*-1,2,3-triazole) (H_2BDTri).[11] Herein, we report two new flexible microporous metal–organic frame-

[a] Dr. A. Demessence, Prof. J. R. Long
Department of Chemistry, University of California
Berkeley, Berkeley CA, 94720-1460 (USA)
Fax: (+1) 510-643-3546
E-mail: jrlong@berkeley.edu

Supporting information for this article is available on the WWW under http://dx.doi.org/10.1002/chem.201000053.

works, Cu(BDTri)L, of the same structure type, but with different coordinated solvent molecules, L = DMF and diethylformamide (DEF), directed toward the cavity interiors. Due to the high stability of the triazolate-bridged framework, the structural transformations through single-crystal to single-crystal conversions can be fully characterized. We then examine how the cavity modifications affect the gate opening and consequently the ability of the material to adsorb N_2 and O_2. The two-step isotherms associated with the breathing of the framework reveals a high gas selectivity, depending on the coordinated solvent.

Results and Discussion

The reaction between $CuCl_2 \cdot 2H_2O$ and H_2BDTri in an acidic mixture of DMF at 120 °C affords the porous metal–organic framework $Cu(BDTri)(DMF) \cdot 1.2H_2O$ (**1a**). X-ray analysis of the green block-shaped crystals showed that the compound crystallizes in the orthorhombic system, adopting space group *Imma* with cell parameters of $a = 22.538(1)$, $b = 7.044(3)$, $c = 13.772(6)$ Å, and $V = 2186.5(2)$ Å^3. The compound is isostructural to Cu(BDT)(DMF) (BDT^{2-} = 1,4-benzeneditetrazolate),[10a] exhibiting a framework wherein octahedral Cu^{II} centers are bridged through a combination of two triazolate groups and a DMF molecule to form one-dimensional chains (Figure 1). Neighboring chains are connected through $BDTri^{2-}$ ligands to form an extended three-dimensional network with one-dimensional channels running along the [010] direction (Figure 2).

Upon exposure of a single crystal of **1a** to ambient atmosphere, its color changed from green to blue (**1b**) after 10 days, and then after 1 month to gray (**1c**). Remarkably, the crystal remained intact throughout these changes, enabling the structures of **1b** and **1c** to be determined. X-ray analyses revealed two new crystallographic forms, wherein the framework connectivity and space group are maintained, with unit cell parameters of $a = 23.739(4)$, $b = 7.0724(1)$, $c = 11.5405(2)$ Å and $V = 1937.5(5)$ Å^3 for **1b**, and $a = 24.561(3)$, $b = 6.9860(9)$, $c = 9.1333(1)$ Å and $V = 1567.1(4)$ Å^3 for **1c** (Figure 2 and Table 1). The change from **1a** to **1c** implies an increase of more than 2 Å of the a axis and a drastic decrease of the c parameter by more than 4.5 Å (while the b parameter remains almost unchanged) and is accompanied by a reduction in the cell volume of 11 and 28% for **1b** and **1c**, respectively. The shrinkage of the framework is due to the release of uncoordinated guest solvent molecules from

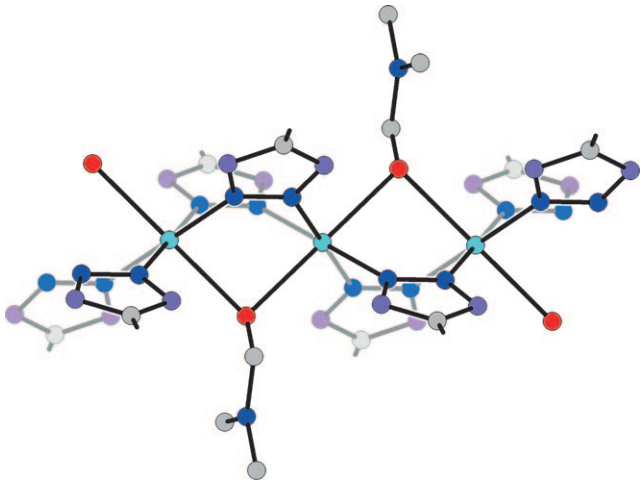

Figure 1. A portion of the crystal structure of **1a**, showing part of a one-dimensional chain. Light blue, red, blue, and gray spheres represent Cu, O, N, and C atoms, while purple spheres represent positions that are either a N or a C atom of a triazolate ring; H atoms are omitted for clarity.

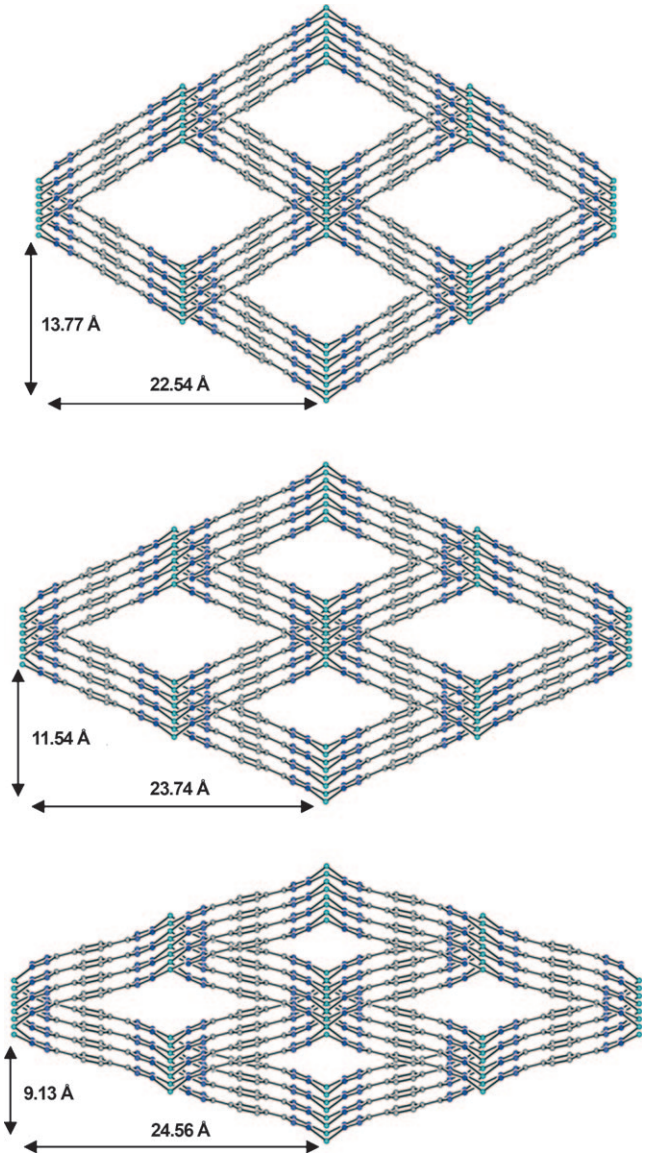

Figure 2. Views of the crystal structures of **1a**, **1b** and **1c** (from up to down) showing the one-dimensional channels along the [010] direction. Light blue, blue, and gray spheres represent Cu, N, and C atoms, while purple spheres represent positions that are either a N or a C atom of a triazolate ring; H atoms and bridging DMF molecules are omitted for clarity.

Table 1. Unit cell parameters, cell volume, and angles, α and β, between the phenyl and the triazolate rings and between the phenyl ring and the plane formed by two copper ions (Cu1) and two bridging nitrogen atoms (N1) from a triazolate function, respectively.

	1a	1b	1c
a [Å]	22.538(1)	23.739(4)	24.561(3)
b [Å]	7.044(3)	7.0724(1)	6.9860(9)
c [Å]	13.772(6)	11.5405(2)	9.1333(1)
V [Å^3]	2186.5(2)	1937.5(5)	1567.1(4)
α [°]	0.671(2)	2.481(2)	8.491(2)
β [°]	0.262(1)	9.223(2)	20.162(2)

the pores of the structure, as observed previously for reversible expanding/shrinking frameworks.[12]

Two explanations have been proposed to describe such breathing behavior.[13] The first is related to the host–guest interactions and the second to the intrinsic flexibility of the framework itself, which is induced by the existence of weak points within the skeleton, allowing the deformation of the network under the action of a stimulus. Such a deformation of the framework structure is usually associated with the modifications of the bridging ligands[14] and/or metal coordination sphere (solvent removal, elongation of bonds).[15] In **1a–c**, however, the position of the atoms around the Cu^{II} centers remains geometrically almost invariant (bond lengths and angles vary by just 0.04 Å and 2°, respectively) and consequently is not responsible for the structural deformations. Instead, the deformation of the framework is mostly explained by the geometry changes associated with flexing of the bridging ligand (Figure 3). In **1a**, the ligand

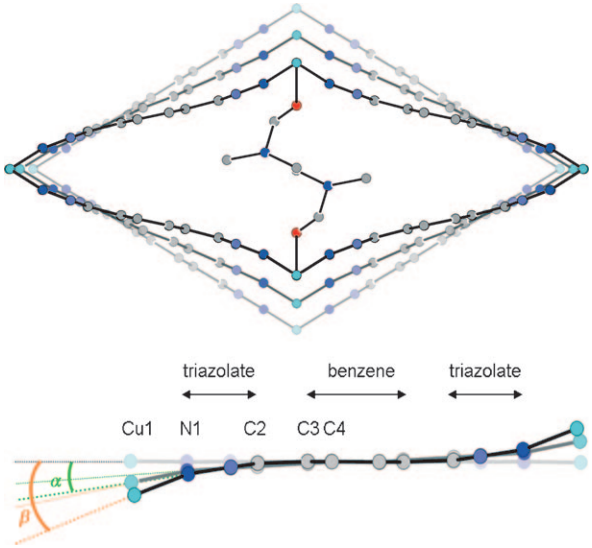

Figure 3. View of the structural deformations upon desolvation of the pores from **1a** (light colors) to **1c** (dark colors). Light blue, red, dark blue, and gray spheres represent Cu, O, N, and C atoms, while blue spheres represent positions that are either a N or a C atom of a triazolate ring; H atoms are omitted for clarity. The projection is along the [010] direction with an edge-on view of the $BDTri^{2-}$ ligands bridging between Cu^{II} centers. The angles *α* and *β* are the angles between the benzene and triazolate rings and the benzene ring and the plane formed by two copper atoms (Cu1) and two coordinated nitrogen atoms (N1) from a triazolate group, respectively.

formed by aromatic rings is planar, but upon desolvation and reduction in the unit cell volume, two phenomena occur to minimize the lattice energy and explain the large shrinkage. First, both triazolate rings of one ligand are bending, one up and one down, to make an angle of 8.491(2)° with the benzene ring in **1c** (Table 1 and Figure 3). Since the triazolate and phenyl rings are planar, this angle is mostly explained by bending at the C2 carbon atoms of the triazolate groups which produce an angle strain, similar to the curved graphene sheets forming fullerenes, for example.[16] This case represents the first characterization of the bending of a sp^2 carbon atom in a small cyclic organic molecule induced by a framework. In addition to this deformation, the bridging nitrogen atoms of the triazolate rings act as a "kneecap" around the Cu···Cu axis, with the angle *β* varying from 0.3(1)° in **1a** to 20.2(2)° in **1c** (Figure 3). Thus, these structural deformations explain the movement of the copper atoms by a distance of 2.319 Å along the [001] axis between the structures of **1a** and **1c**. Presumably, the steric repulsion between the methyl groups of the coordinated DMF molecules and the C2 carbon atoms of the triazolate rings (C2···C6 = 3.4(4) Å) prevent the collapsing of the framework and any further shrinkage. In addition, the strong bond between the triazolate rings and the metal ions is likely to enable the observation of multiple single-crystal transformations,[15b] allowing us to identify a new example of framework flexibility associated primarily with bending of the bridging rigid ligands. Moreover, the coordinated DMF molecules extending into the pores act as pillars between the copper chains to maintain a permanent microporosity.

Powder X-ray diffraction patterns allowed a study of the structural dynamics associated with the flexibility of the framework to be performed. In Figure 4a the diffraction pattern for a freshly prepared sample of **1c** upon drying under vacuum is displayed. Addition of water to the sample induces an immediate change in the pattern, corresponding to the regeneration of the structure of **1a** upon incorporation of guest water molecules. Leaving the framework in air at room temperature for only a few minutes then leads to a reverse to the closed structure of **1c** through release of the water molecules. A similar breathing effect was observed when the sample was treated with methanol instead of water (Figure 4e). During the reversible transformations, the peaks of the powder diffraction patterns exhibit drastic but continuous displacements that are characteristic of a breathing effect, without loss of crystallinity after several desolvation-resolvation cycles. These tests demonstrate the chemical stability of the framework in solvents such as water and methanol, as well as structural stability through the course of multiple breathing events.

To investigate the flexible nature of the compound, we measured the H_2, N_2, and O_2 adsorption isotherms at 77 K (Figure 5). The H_2 isotherm reveals a reversible excess uptake of 3.6 mmol g^{-1} (0.77 wt %), which did not increase significantly at higher pressures of up to 100 bar. The N_2 and O_2 isotherms are characterized by two distinct adsorption steps and marked hysteresis, which is related to the flexibili-

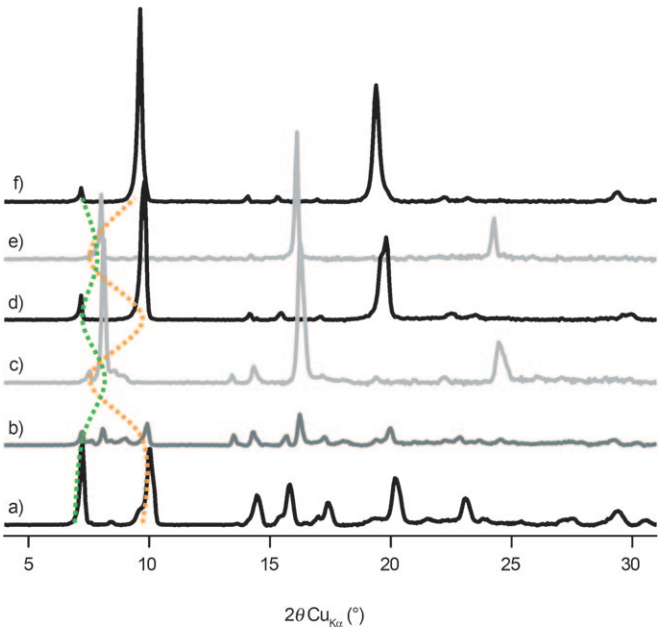

Figure 4. Powder X-ray diffraction patterns of different phases observed for Cu(BDTri)(DMF). a) Structure **1c** upon drying under vacuum, b) at $t=1$ min after adding a drop of H_2O, c) at $t=15$ min (**1a**), d) at $t=40$ min (**1c**), e) at $t=45$ min after adding a drop of MeOH (**1a**), and f) at $t=75$ min (**1c**). The orange and green dotted lines correspond to the evolution of the positions of the 101 and 200 reflections, respectively.

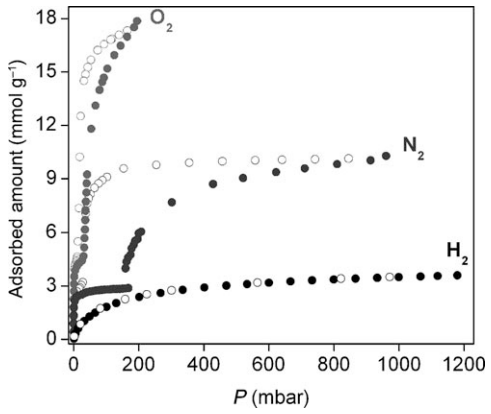

Figure 5. Gas adsorption isotherms for the uptake of N_2, H_2, and O_2 in Cu(BDT)(DMF) at 77 K.

ty of the framework. After a steep rise at low pressure, the N_2 isotherm reaches a plateau. The amount of adsorbed gas at this first step (0.100 mL g^{-1} at 168 mbar) is in good agreement with the void volume of **1c** calculated from the crystal structure (0.108 mL g^{-1}) and can be attributed to the permanent porosity of the phase. A Langmuir fit to the first step of the N_2 adsorption data gives an apparent surface area of 330 m^2 g^{-1}. At higher pressure, the amount of N_2 adsorbed in the second step reaches 3.5 times that of the first step. At 77 K and 960 mbar, the adsorbed amount of N_2 of 0.357 mL g^{-1} corresponds more closely to the void volume of **1b** (0.337 mL g^{-1}) than to that of **1a** (0.458 mL g^{-1}), suggesting that the framework is not completely opened at this pressure. The Langmuir surface area obtained by fitting the linear part of the isotherm in the high-pressure range is 1160 m^2 g.[17] Therefore, the first step of this two-step N_2 adsorption isotherm is related to the structure of **1c** in which the DMF molecules act as pillars to leave a permanent microporosity, whereas the second step apparently originates from the pore opening of the framework. Although many metal–organic frameworks exhibiting a structural change prompted by external stimuli display multi-stepwise gas adsorption isotherms,[5a] the phenomena are usually related to a "blocking effect"[18] or to a "breathing effect".[19] To the best of our knowledge, the present case represents only the second example in which this kind of gas adsorption is associated with the presence of rigid micropores due to the pillaring role of anions or solvent molecules, followed by a pore opening process.[20]

The two-step O_2 adsorption isotherm at 77 K, compared with the N_2 adsorption isotherm, shows a larger amount of adsorbed gas and a lower pressure for the pore opening. The first step, similar to that of N_2, is characterized by a steep rise at low pressure, related to the microporosity of **1c**. The number of gas molecules adsorbed at the plateau is approximately 1.6 times the number of N_2 molecules adsorbed, in line perhaps with the smaller kinetic diameter of O_2 (3.46 Å) relative to N_2 (3.64 Å).[21] The second O_2 adsorption step, governed by the pore-opening process, arises at a lower pressure than for N_2, which correlates with the expected strength of interactions with a surface, as reflected in the different boiling points of the molecules ($N_2=77$ K, $O_2=90$ K).[5b] The much larger amount of adsorbed O_2 gas associated with the second step (17.8 mL g^{-1} at 195 mbar) seems to correspond to the available pore volume of structure **1a** instead of **1b**. Thus, the interaction/repulsion of guest gas molecules with the surfaces of the framework, and their gate-opening ability, cannot be excluded as a determining factor for the adsorption selectivity. In considering other possible reasons for the larger amount of O_2 adsorbed, factors such as the paramagnetism of O_2 and the greater quadrupole moment of N_2 could also potentially play a role.[6,22]

At 168 mbar, O_2 molecules are adsorbed more favorably (17.0 mL g^{-1}) than N_2 molecules (2.9 mL g^{-1}) with a selectivity of 5.9:1. To the best of our knowledge, only a few other metal–organic frameworks have been shown to exhibit a similar effect with these gases at low pressure.[10,23] While this ratio is not the highest reported, it represents a good compromise between the selectivity ratio and the quantity of adsorbed gas. For example, $Yb_4(\mu_4\text{-}H_2O)$(4,4′,4″-S-triazine-2,4,6-triyl-tribenzoate)$_{8/3}(SO_4)_2\cdot 3\,H_2O\cdot 10$ DMSO has the highest selectivity ratio ≈9.4:1, but a low quantity of adsorbed O_2 (9.4 mL g^{-1} of adsorbed O_2 at 201 mbar and 77 K)[24] and $\{Ag_2[Ag_4\text{-}(3,5\text{-bis(trifluoromethyl)-1,2,4-triazolate})_6]\}_n$ exhibits a large capacity for O_2 uptake (21 mmol g^{-1} at 30 mbar and 77 K), but a relatively poor O_2/N_2 selectivity of 1.2:1.[25] Both N_2 and O_2 isotherms show hysteresis loops associated with a two-step desorption process. Indeed, the

open phase is maintained until the pressure drops to 50 and 30 mbar for N_2 and O_2, respectively. The low-pressure plateau in the desorption curves can be attributed to adsorbent–adsorbate or adsorbate–adsorbate interactions through van der Waals forces until the framework releases sufficient gas molecules to allow pore closing, after which the amount of gas adsorbed drops precipitously.[17] This second desorption step is due to the permanent microporosity of **1c**, similar to what is observed for rigid frameworks. Adsorption measurements of N_2 and O_2 gas molecules at 87 K show that the pressure needed to open the pores increases as the temperature increases (Figure S3 in the Supporting Information). For N_2 adsorption the pressure of pore opening is shifted from 170 to 570 mbar for experiments at 77 and 87 K, respectively, while for O_2 adsorption, the shift is from 30 to 180 mbar at the same temperatures. Such behavior has been previously observed with different gases in several flexible metal–organic frameworks, and has been explained as relating to the rate at which the gas molecules strike the solid surface under supercritical conditions.[5]

To study the effect of the solvent molecules pointing into the channel-like pores of the structure on the pore opening for O_2/N_2 gas adsorption, the compound was synthesized in DEF instead of DMF. The powder X-ray diffraction pattern of the resulting framework, corresponding to a formula of Cu(BDTri)(DEF), matches that of the intermediate open phase of Cu(BDTri)(DMF) (**1b**), indicating that the frameworks of these two materials are identical, but with different bridging solvent molecules (Figure S4 in the Supporting Information). Prior to measuring H_2, N_2, and O_2 gas adsorption isotherms, this compound was degassed by heating at 120 °C under dynamic vacuum. As shown in Figure 6, the H_2 adsorption isotherm at 77 K reveals a reversible uptake of 2.3 mmol g^{-1} (0.46 wt %) at 1.2 bar. This represents a lower value than the DMF-based Cu(BDTri) framework, consistent with the greater volume occupied by the bridging DEF molecules, which reduces the pore volume of the closed phase (analogous to **1c**). Interestingly, the N_2 adsorption isotherm at 77 K does not display two steps, but rather a type I curve indicating a BET surface area of 100 $m^2 g^{-1}$. This reduced surface area can also be explained by the presence of the larger DEF solvent molecules within the closed framework structure. As for Cu(BDT)(DMF)[10a] and Cu(BDTri)(DMF), the O_2 adsorption isotherm measured at 77 K for Cu(BDTri)(DEF) reveals a two-step adsorption process. A Langmuir fit to the low-pressure step of the isotherm gives an estimated surface area of 240 $m^2 g^{-1}$. The second step, much more significant, occurs at 50 mbar and corresponds to adsorption of 15.9 mmol g^{-1} of O_2 at 200 mbar. At this pressure the selectivity of O_2 over N_2 reaches 13.5, by far surpassing the value of the isostructural compounds Cu(BDT)(DMF) and Cu(BDTri)(DMF) and representing the highest value yet observed for a microporous material under similar conditions. It also represents an initial demonstration of how changing the molecules bound at the surface within a flexible metal–organic framework can dramatically affect the gas adsorption selectivity.

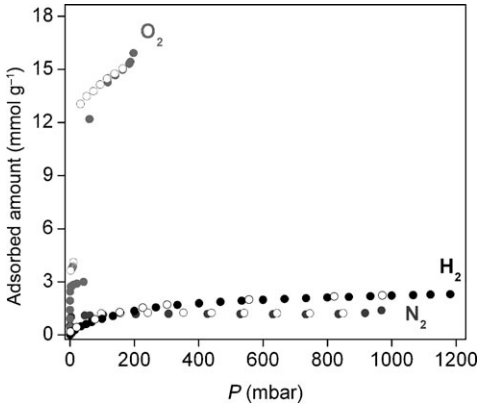

Figure 6. Gas adsorption isotherms for the uptake of N_2, H_2, and O_2 in Cu(BDTri)(DEF) at 77 K.

This work shows a rare example of selective two-step gas adsorption at low pressure associated with the flexibility of the framework and coupled with a guest-dependent gate-opening pressure.[26]

Conclusion

These results demonstrate the successful incorporation of the new bridging ligand $BDTri^{2-}$ in the flexible metal–organic frameworks Cu(BDTri)(L) (L = DMF, DEF). Due to the strong bonds between the triazolate rings and the Cu^{II} centers, the initial and final stages of breathing could be characterized, together with an intermediate state, leading to a detailed understanding of the structural deformations associated with framework breathing. Here, deformation of the ligand coupled with the ability of the triazolate ring to act as a kneecap is responsible for the reversible flexibility. The bending at an sp^2 carbon atom in triazolate function has no analogue in carboxylate-based frameworks. Hence, it appears that the use of triazolate-based ligands can provide a new way of generating flexible frameworks.

The Cu(BDTri)(DMF) framework also shows two-step isotherms at 77 K for the adsorption of O_2 and N_2, which is associated with the permanent microporosity of the closed phase and a pore-opening process. Moreover compared with the isostructural tetrazolate-based framework Cu(BDT)(DMF),[10a] a significant improvement in the amount of gas taken up is observed. With larger DEF bridging molecules, the analogous framework Cu(BDTri)(DEF) exhibits a selective pore opening with O_2 but not with N_2 gas. This observation points to the importance of how adjusting the nature of coordinated solvent molecules on a framework surface can lead to control over selectivity and the pressure required to induce pore opening. This selective breathing has implications for a range of potential applications, including stereospecific chemical catalysis, molecular separations, and chemical sensing. It is important to emphasize, however, that while these materials are of significant interest for understanding selective gas interactions within metal–organic

frameworks, they are unlikely to find utility in performing O_2/N_2 separations owing to 1) the low temperatures required (at 298 K and 1.2 bar, the O_2 adsorbed in Cu(BDTri)(DMF) drops to 0.03 mmol g^{-1} (Figure S5 in the Supporting Information)) and 2) the fact that pore opening induced by one component of a mixture of gases is also likely to enable entry for other components of similar size.

Experimental Section

General: All reagents were obtained from commercial vendors and used without further purification. The compound 1,4-diethynylbenzene was synthesized according to a previously published procedure (see the Supporting Information).[27]

H_2BDTri·2H_2O: Trimethylsilyl azide (5.2 g, 45 mmol) was added to a solution of DMF and MeOH (60 mL, 9:1) containing CuI (286 mg, 1.5 mmol) and 1,4-diethynylbenzene (1.9 g, 15 mmol) under a nitrogen atmosphere. The reaction mixture was stirred at 90 °C for 44 h. The mixture was cooled to room temperature, filtered, and concentrated. Water (30 mL) was added to the filtrate to obtain the product as a pale yellow precipitate. The solid was washed with Et_2O and dried under vacuum to yield the product (2.6 g, 82 %). ^{1}H NMR (300 MHz, $(CD_3)_2SO$): $\delta = 15.03$ (s, 1H), 8.31 (s, 1H), 7.95 ppm (s, 2H). IR (neat): $\tilde{\nu} = 3155$, 3115, 2960, 2865, 1655, 1460, 1430, 1370, 1355, 1335, 1310, 1225, 1200, 1135, 1080, 1005, 970, 875, 845, 730, 705, 650 cm^{-1}; elemental analysis calcd (%) for $C_{10}H_8N_6$·2H_2O: C 48.38, H 4.87, N 33.85; found: C 48.58, H 4.88, N 33.80.

Cu(BDTri)(DMF)·1.2H_2O: A mixture of solutions of $CuCl_2$·2H_2O (0.075 M, 0.15 μmol) in DMF (200 μL) and H_2BDTri·2H_2O (0.075 M, 0.15 μmol) in DMF (200 μL) was titrated with dilute HNO_3 until the pH of the solution reached 4. The mixture was heated in a 2 mL scintillation vial sealed with a Teflon-lined cap at 80 °C for 48 h. The resulting green crystals were collected by filtration and found to be suitable for single-crystal X-ray analysis. For larger scales, a mixture of solutions of $CuCl_2$·2H_2O (0.10 μg, 0.59 mmol) in DMF (15 mL) and of H_2BDTri·2H_2O (140 mg, 0.56 mmol) in DMF (15 mL) was titrated with dilute HNO_3 until the pH of the solution reached 4. The mixture was heated in a 125 mL scintillation vial sealed with a Teflon-lined cap at 80 °C for 48 h. The resulting powder was collected by filtration, washed with DMF, and dried under reduced pressure to yield the product (150 mg, 73 %). IR (neat): $\tilde{\nu} = 3335$, 2925, 2855, 1660, 1490, 1475, 1435, 1415, 1390, 1235, 1215, 1155, 1100, 1060, 985, 825, 665 cm^{-1}; elemental analysis calcd (%) for $C_{13}H_{14.4}CuN_7O_{2.2}$: C: 42.11, H: 4.74, N: 26.44; found C:42.11, H: 3.69, N: 26.69.

Cu(BDTri)(DEF)·0.9H_2O: A mixture of solutions of $CuCl_2$·2H_2O (0.10 μg, 0.59 mmol) in DEF (15 mL) and of H_2BDTri·2H_2O (140 mg, 0.56 mmol) in DEF (15 mL), was titrated with dilute HNO_3 until the pH of the solution reached 4. The mixture was heated in a 125 mL scintillation vial sealed with a Teflon-lined cap at 80 °C for 48 h. The powder was collected by filtration, washed with DEF, and dried under reduced pressure to yield the product (135 mg, 62 %). IR (neat): $\tilde{\nu} = 3245$, 2975, 2935 2880, 1650, 1495, 1475, 1435, 1415, 1385, 1250, 1210, 1150, 1105, 1060, 985, 835, 665 cm^{-1}; elemental analysis calcd (%) for $C_{15}H_{17.8}CuN_7O_{1.9}$: C: 41.99, H: 3.48, N: 29.61; found C:42.01, H: 3.15, N: 29.89.

Gas adsorption measurements: Gas adsorption isotherms for pressures in the range 0–1.2 bar were measured by using a Micromeritics ASAP2020 instrument. Powders of the compounds Cu(BDTri)(L) (L = DMF, DEF) were transferred to a preweighed analysis tube, which was capped with a Transeal and evacuated by heating at 120 °C under dynamic vacuum until an outgas rate of less than 2 mtorr min^{-1} (0.27 Pa min^{-1}) was achieved. The powder X-ray diffraction patterns of the desolvated frameworks correspond to the collapsed framework structure **1c**. (Attempts to remove the coordinating DMF molecules in **1c** by heating at 0.2 °C min^{-1} to temperatures between 120 and 250 °C did not change the surface area, while at 270 °C the framework lost its crystallinity) The evacuated analysis tubes containing the degassed samples were transferred to an electronic balance and weighed again to determine the mass of sample (94.7 and 41.3 mg for L = DMF and DEF, respectively). The tube was then transferred back to the analysis port of the gas adsorption instrument. The outgas rate was again confirmed to be less than 2 mtorr min^{-1} (0.27 Pa min^{-1}). For all isotherms, warm and cold free-space correction measurements were performed by using ultra-high purity He gas (UHP grade 5.0, 99.999 % purity). The N_2, O_2, and H_2 isotherms at 77 K were measured in a liquid nitrogen bath, using UHP-grade gas sources. The N_2 and O_2 gas adsorption experiments were paused after 50 h to refill the liquid nitrogen bath (time of full experiment around 4 d). Oil-free vacuum pumps and oil-free pressure regulators were used for all measurements to prevent contamination of the samples during the evacuation process, or of the feed gases during the isotherm measurement.

X-ray structure determinations: Crystals, coated in Paratone-N oil and attached to Kapton loops, were transferred to a Siemens SMART APEX diffractometer (**1a** and **1b**) or to a Bruker Platinum 200 Instrument at the Advanced Light Source at the Lawrence Berkeley National Laboratory (**1c**), and cooled in a nitrogen stream. Lattice parameters were initially determined from a least-squares analysis of more than 100 centered reflections; these parameters were later refined against all data. None of the crystals showed significant decay during data collection. The raw intensity data were converted (including corrections for background, Lorentz, and polarization effects) to structure factor amplitudes and their esds by using the SAINT 7.07b program. An empirical absorption correction was applied to each data set by using SADABS. Space-group assignment was based on systematic absences, *E* statistics, and successful refinement of the structures. Structures were solved by direct methods with the aid of difference Fourier maps and were refined against all data by using the SHELXTL 5.0 software package. Hydrogen atoms were inserted at idealized positions and refined by using a riding model with an isotropic thermal parameter 1.2 times that of the attached carbon atom. The disorder evident in the electron-density map prevented the refinement of solvent molecules within the pores of **1a** and **1b**. As such, all peaks with electron densities larger than one electron were refined as partially occupied O and C atoms. CCDC-755760, 755761, and 755762 contains the supplementary crystallographic data for this paper. These data can be obtained free of charge from The Cambridge Crystallographic Data Centre via www.ccdc.cam.ac.uk/data_request/cif.

Other physical measurements: Infrared spectra were collected on a Nicolet Avatar 360 FTIR spectrometer with an attenuated total reflectance accessory. ^{1}H NMR spectra were obtained by using a Bruker AVQ-400 instrument. Elemental analyses were obtained from the Microanalytical Laboratory of the University of California, Berkeley. Powder X-ray diffraction patterns were recorded using $Cu_{K\alpha}$ radiation ($\lambda = 1.5406$ Å) on a Bruker D8 Advance diffractometer. Thermogravimetric analyses were carried out at a ramp rate of 1 °C min^{-1} in a nitrogen flow with a TA Instruments TGA Q5000 V3.1 Build 246 instrument.

Acknowledgements

This research was supported by General Motors, Inc., and as part of the Center for Gas Separations Relevant to Clean Energy Technologies, an Energy Frontier Research Center funded by the U.S. Department of Energy, Office of Science, Office of Basic Energy Sciences under Award Number DE-SC0001015. We thank Dr. H. J. Choi, Dr. D. M. D'Alessandro, and Dr. S. Horike for helpful discussions. A portion of this research was conducted at the Advanced Light Source facility at the Lawrence Berkeley National Laboratory, which is operated by the DoE under Contract DE-AC03-76SF00098.

[1] a) S. Kitagawa, R. Kitaura, S. Noro, *Angew. Chem.* **2004**, *116*, 2388; *Angew. Chem. Int. Ed.* **2004**, *43*, 2334; b) K. Uemura, R. Matsuda, S. Kitagawa, *J. Solid State Chem.* **2005**, *178*, 2420; c) A. J. Fletcher, K. M. Thomas, M. J. Rosseinsky, *J. Solid State Chem.* **2005**, *178*,

2491; d) D. Bradshaw, J. E. Warren, M. J. Rosseinsky, *Science* **2007**, *315*, 977; e) C. Serre, C. Mellot-Draznieks, S. Surblé, N. Audebrand, Y. Filinchuk, G. Férey, *Science* **2007**, *315*, 1828; f) G. Férey, C. Serre, *Chem. Soc. Rev.* **2009**, *38*, 1380.

[2] a) P. L. Llewellyn, S. Bourrelly, C. Serre, Y. Filinchuk, G. Férey, *Angew. Chem.* **2006**, *118*, 7915; *Angew. Chem. Int. Ed.* **2006**, *45*, 7751; b) T. K. Maji, R. Matsuda, S. Kitagawa, *Nat. Mater.* **2007**, *6*, 142.

[3] Y. Kubota, M. Takata, R. Matsuda, R. Kitaura, S. Kitagawa, T. C. Kobayashi, *Angew. Chem.* **2006**, *118*, 5054; *Angew. Chem. Int. Ed.* **2006**, *45*, 4932.

[4] G. J. Halder, C. J. Kepert, B. Moubaraki, K. S. Murray, J. D. Cashion, *Science* **2002**, *298*, 1762.

[5] a) H. J. Choi, M. Dincă, J. R. Long, *J. Am. Chem. Soc.* **2008**, *130*, 7848; b) D. Tanaka, K. Nakagawa, M. Higuchi, S. Horike, Y. Kubota, T. C. Kobayashi, M. Takata, S. Kitagawa, *Angew. Chem.* **2008**, *120*, 3978; *Angew. Chem. Int. Ed.* **2008**, *47*, 3914.

[6] J.-R. Li, R. J. Kuppler, H.-C. Zhou, *Chem. Soc. Rev.* **2009**, *38*, 1477.

[7] C. R. Reid, I. P. O'koye, K. M. Thomas, *Langmuir* **1998**, *14*, 2415.

[8] a) M. Dincă, J. R. Long, *J. Am. Chem. Soc.* **2007**, *129*, 11172; b) B. Arstad, H. Fjellvåg, K. O. Kongshaug, O. Swang, R. Blom, *Adsorption* **2008**, *14*, 755; c) M. Dincă, A. Dailly, J. R. Long, *Chem. Eur. J.* **2008**, *14*, 10280.

[9] a) O. K. Farha, K. L. Mulfort, J. T. Hupp, *Inorg. Chem.* **2008**, *47*, 10223; b) A. Demessence, D. M. D'Alessandro, M. L. Foo, J. R. Long, *J. Am. Chem. Soc.* **2009**, *131*, 8784; c) Y.-S. Bae, O. K. Farha, J. T. Hupp, R. Q. Snurr, *J. Mater. Chem.* **2009**, *19*, 2131.

[10] a) M. Dincă, A. F. Yu, J. R. Long, *J. Am. Chem. Soc.* **2006**, *128*, 8904; b) M. Dincă, A. Dailly, Y. Liu, C. M. Brown, D. A. Neumann, J. R. Long, *J. Am. Chem. Soc.* **2006**, *128*, 16876.

[11] T. Jin, S. Kamijo, Y. Yamamoto, *Eur. J. Org. Chem.* **2004**, 3789.

[12] T. Loiseau, C. Serre, C. Huguenard, G. Fink, F. Taulelle, M. Henry, T. Bataille, G. Férey, *Chem. Eur. J.* **2004**, *10*, 1373.

[13] a) S. Kitagawa, K. Uemura, *Chem. Soc. Rev.* **2005**, *34*, 109; b) G. Férey, *Chem. Soc. Rev.* **2008**, *37*, 191.

[14] C. Serre, C. Mellot-Draznieks, S. Surblé, N. Audebrand, Y. Filinchuk, G. Férey, *Science* **2007**, *315*, 1828.

[15] a) D. Bradshaw, J. E. Warren, M. J. Rosseinsky, *Science* **2007**, *315*, 977; b) B. D. Chandler, G. D. Enright, K. A. Udachin, S. Pawsey, J. A. Ripmeester, D. T. Cramb, G. K. H. Shimizu, *Nat. Mater.* **2008**, *7*, 229.

[16] H. W. Kroto, J. R. Heath, S. C. O'Brien, R. F. Curl, R. E. Smalley, *Nature* **1985**, *318*, 162.

[17] R. Kitaura, K. Seki, G. Akiyama, S. Kitagawa, *Angew. Chem.* **2003**, *115*, 444; *Angew. Chem. Int. Ed.* **2003**, *42*, 428.

[18] E.-Y. Choi, K. Park, C.-M. Yang, H. Kim, J.-H. Son, S. W. Lee, Y. H. Lee, D. Min, Y.-U. Kwon, *Chem. Eur. J.* **2004**, *10*, 5535.

[19] C. Serre, S. Bourrelly, A. Vimont, N. A. Ramsahye, G. Maurin, P. L. Llewellyn, M. Daturi, Y. Filinchuk, O. Leynaud, P. Barnes, G. Férey, *Adv. Mater.* **2007**, *19*, 2246.

[20] A. Kondo, H. Noguchi, L. Carlucci, D. M. Proserpio, G. Ciani, H. Kajiro, T. Ohba, H. Kanoh, K. Kaneko, *J. Am. Chem. Soc.* **2007**, *129*, 12362.

[21] D. W. Breck, *Zeolite Molecular Sieves*, Wiley, New York, **1984**.

[22] S. S. Kaye, H. J. Choi, J. R. Long, *J. Am. Chem. Soc.* **2008**, *130*, 16921.

[23] a) D. N. Dybtsev, H. Chun, S. H. Yoon, D. Kim, K. Kim, *J. Am. Chem. Soc.* **2004**, *126*, 32; b) M. Dincă, J. R. Long, *J. Am. Chem. Soc.* **2005**, *127*, 9376; c) S. M. Humphrey, J.-S. Chang, S. H. Jhung, J. W. Yoon, P. T. Wood, *Angew. Chem.* **2007**, *119*, 276; *Angew. Chem. Int. Ed.* **2007**, *46*, 272; d) S. Ma, X.-S. Wang, C. D. Collier, E. S. Manis, H.-C. Zhou, *Inorg. Chem.* **2007**, *46*, 8499; e) J.-R. Li, Y. Tao, Q. Yu, X.-H. Bu, H. Sakamoto, S. Kitagawa, *Chem. Eur. J.* **2008**, *14*, 2771; f) H.-S. Choi, M. P. Suh, *Angew. Chem.* **2009**, *121*, 6997; *Angew. Chem. Int. Ed.* **2009**, *48*, 6865; g) P. L. Llewellyn, P. Horcajada, G. Maurin, T. Devic, N. Rosenbach, S. Bourrelly, C. Serre, D. Vincent, S. Loera-Serna, Y. Filinchuk, G. Férey, *J. Am. Chem. Soc.* **2009**, *131*, 13002.

[24] S. Ma, X.-S. Wang, D. Yuan, H.-C. Zhou, *Angew. Chem.* **2008**, *120*, 4198; *Angew. Chem. Int. Ed.* **2008**, *47*, 4130.

[25] C. Yang, X. Wang, M. A. Omary, *J. Am. Chem. Soc.* **2007**, *129*, 15454.

[26] Z. Wang, S. M. Cohen, *J. Am. Chem. Soc.* **2009**, *131*, 16675.

[27] E. Weber, M. Hecker, E. Koepp, W. Orlia, M. Czugler, I. Csöregh, *J. Chem. Soc. Perkin Trans. 2* **1988**, 1251.

Received: January 9, 2010
Published online: April 15, 2010

